PCTAIRE1 phosphorylates p27 and regulates mitosis in cancer cells

Teruki Yanagi, **Maryla Krajewska**, **Shu-ichi Matsuzawa**, and **John C. Reed**

Abstract

PCTAIRE1 is distant relative of the cyclin-dependent kinase family that has been implicated in spermatogenesis and neuronal development, but it has not been studied in cancer. Here we report that PCTAIRE1 is expressed in prostate, breast, and cervical cancer cells where its RNAi-mediated silencing causes growth inhibition with aberrant mitosis due to defects in centrosome dynamics. PCTAIRE1 was not similarly involved in proliferation of non-transformed cells including diploid human IMR-90 fibroblasts. Through yeast two-hybrid screening we identified tumor suppressor p27 as a PCTAIRE1 interactor. In vitro kinase assays showed PCTAIRE1 phosphorylates p27 at Ser10. PCTAIRE1 silencing modulated Ser10 phosphorylation on p27 and led to its accumulation in cancer cells but not in non-transformed cells. In a mouse xenograft model of PPC1 prostate cancer, conditional silencing of PCTAIRE1 restored p27 protein expression and suppressed tumor growth. Mechanistic studies in HeLa cells showed that PCTAIRE1 phosphorylates p27 during the S and M phases of the cell cycle. Notably, p27 silencing was sufficient to rescue cells from mitotic arrest caused by PCTAIRE1 silencing. Clinically, PCTAIRE1 was highly expressed in primary breast and prostate tumors compared to adjacent normal epithelial tissues. Together our findings reveal an unexpected role for PCTAIRE1 in regulating p27 stability, mitosis and tumor growth, suggesting PCTAIRE1 as a candidate cancer therapeutic target.

Introduction

PCTAIRE1 (also known as cyclin-dependent kinase 16 (Cdk16) and PCTK1) is a member of the PCTAIRE family, a group of kinases related to the Cdk family, which includes PCTAIRE-1, 2, and 3 (1). PCTAIRE1 is broadly expressed, with highest levels in the brain and testis (2). Demonstrated functions for PCTAIRE1 include vesicular exocytosis and protein secretion, neuronal migration, neurite outgrowth, and spermatogenesis (3–7). PCTAIRE1 has a central kinase domain that has amino acid sequence similarity to other Cdk family members, and is flanked by unique N-terminal and C-terminal domains. While PCTAIRE1 contains a motif reminiscent of cyclin binding sites found in other Cdk family members (1), the mechanisms responsible for its activation are only partly understood (1, 8). Interaction of the PCTAIRE1 N-terminal domain with cyclin Y stimulates its kinase activity

---

Correspondence to either: John C. Reed or Shu-ichi Matsuzawa, Sanford-Burnham Medical Research Institute, 10901 North Torrey Pines Road, La Jolla, CA 92037, USA, TEL: +1- 858-795-5252, FAX: +1-858-646-3199, smatsuzawa@sanfordburnham.org or reedoffice@sanfordburnham.org.

(6), while PCTAIRE1 binding to the Cdk5 activator does not result in PCTAIRE1 activation (9). Furthermore, some transformed cells express elevated levels of PCTAIRE1 (10).

p27 (also known as Kip1, cyclin-dependent kinase inhibitor 1B) is a tumor suppressor that regulates cell proliferation, cell motility and apoptosis (11). Consistent with a tumor suppressor role for p27, loss of nuclear p27 is frequently observed in human malignancies and is associated with high-grade tumors and poor prognosis (11, 12). In contrast to conventional tumor suppressors such as p53, loss of p27 expression commonly occurs not through genetic mutations or epigenetic silencing, but rather via increased proteosomal degradation or relocalization (11, 13, 14). Thus, increased rates of degradation and elevated rates of nuclear export are thought to cause the decreased nuclear levels of p27 seen in tumor cells.

We report here investigations of the role of PCTAIRE1 in tumorigenesis, which provide evidence that PCTAIRE1 plays an indispensable role in proliferation of some types of cancer cells. PCTAIRE1-depleted cancer cells show mitotic arrest associated with centrosome dysregulation. PCTAIRE1 also directly binds p27, and phosphorylates it at Ser10, thereby promoting degradation of this tumor suppressor. In tumor xenografts, conditional knockdown of PCTAIRE1 restored p27 protein expression and suppressed tumor growth. In addition, analysis of primary tumors from patients revealed elevated levels of PCTAIRE1 in many prostate and breast cancers. Taken together, these findings reveal an unexpected role for PCTAIRE1 in cancer cell division, thus suggesting that this kinase may provide a novel target for future discovery of oncology therapeutics.

Material and Methods

Cell lines and cell culture

PPC1, Du145, MDA-MB-468, T47D, MCF7, IMR-90, HeLa, and HEK293T cells were purchased from ATCC. 267B1 and 267B1/K-ras were kind gifts from Dr. Dritschilo (15). All cells were used in fewer than six months of continuous passage.

Reagents and antibodies

Pre-designed small interfering RNA (siRNA) directed against human Cdk1 (s464), Cdk5 (s2825), PCTAIRE1 (1472, 1566, 1656), p27 (s2837), and negative scramble control (#1, #2), were purchased from Life Technologies. Kinase inhibitors (SNS-032 and ABT-869) were purchased from Selleckchem. Antibodies against PCTAIRE1 (mouse: G6.1 Santa cruz, or rabbit: HPA001366 Sigma), pro-caspase 3 (#9662, Cell Signaling), cleaved caspase 3 (#9661, Cell Signaling), cleaved PARP (mouse, Cell Signaling), p27 (mouse G173-524: BD, or rabbit C-19: Santa Cruz), phospho-p27 Ser10 (sc-12939, Santa Cruz), phospho-p27 Thr187 (37-9700, Invitrogen), phospho-p27 Thr198 (AF3994, R and D), Lamin-B1 (Invitrogen), phospho-Histone H3 (D2C8, Cell Signaling), Eg5 (611186, BD), Cdk1 (610037, BD), Cdk2 (610145, BD), Cyclin B1 (#4138, Cell Signaling), phospho-cdc2 (Y15) (#9111, Cell Signaling), pericentrin (ab4448, Abcam), alpha-tubulin (T5168, Sigma), HA (3F10, Roche), Myc (Roche), beta-actin (Sigma), horseradish-peroxidase (HRP)-conjugated

secondary antibodies (GE Health Care), and Alexa Fluor 488/594-conjugated secondary antibodies (Life Technologies) were purchased from the indicated sources.

Plasmids

Point mutations of PCTAIRE1 (K194M) and p27 (S10A, T187A, T198A) were generated by a PCR-based site directed mutagenesis method. Expression plasmids for various proteins were constructed in the pcDNA3 vector for transfection or the pET vector for generating recombinant proteins.

RNA interference

For transient knockdown, cells were transfected with siRNA duplexes by a reverse transfection method using Lipofectoamine RNAiMAX.

Extraction of total RNA and quantitative RT-PCR analysis

Total RNA were isolated from cultured cells and xenograft tumors using the RNeasy plus mini kit (Qiagen). We reverse-transcribed RNA using Superscript III (Life Technologies) according to the manufacturer's instructions. Complementary DNA samples were analyzed by the SYBR green system (Promega). The sequences for primers are described in supplementary Materials and Methods.

Laemmli SDS-PAGE, Phos-tag SDS-PAGE, immunoblotting and immunoprecipitation

Laemmli SDS-PAGE, immunoblotting and immunoprecipitation were performed as previously described (14). Phos-tag SDS-PAGE was performed with precast phostag gels according to the manufacturer's protocol (Wako Chemical). To distinguish cytosolic and nuclear proteins, cells were fractionated using Nuclear Extract Reagents (Active motif) according to the manufacturer's protocol.

Cell viability assays using ATP measurement

Cells were plated at a density of 5,000–10,000 cells per well, and cultured for 48 or 72 hours. Cell Titer Glo solution (Promega) was added at 100 µl per well and the plates were kept in the dark for 15 minutes before reading the luminescence with a luminometer (Luminoskan Ascent; Thermo Scientific Corporation).

Cell growth assay

To measure cell growth rates, $0.5–1.0 \times 10^5$ cells with Tet-inducible shRNA were plated onto 60 mm diameter plates. After 1 day, culture media was changed to that with (ON) or without (OFF) doxycycline (100 ng/ml). The numbers of cells were counted 1, 3, 5, and/or 7 days after seeding. In siRNA experiments, the number of cells was counted 2 or 3 days after transfection.

Clonogenic assay

Cells with Tet-inducible shRNA were seeded at 300–1,000 cells per well in 35 mm dishes. Cells were cultured with (ON) or without (OFF) doxycycline for 10–14 days. After fixation

by methanol, cells were incubated with 0.5% crystal violet dye. A colony was defined as consisting of at least 50 cells.

Cell cycle analysis by FACS

Cells were fixed with cold 70% ethanol, and suspended in 100 μl of PBS containing 0.5 μl of phospho-Histone H3 antibody incubated for 1 hour. After washing by PBS, cells were incubated for 30 minutes with Alexa488-conjugated secondary antibodies. Cells were treated with propidium iodide (20 μg/ml) and ribonuclease A (10 μg/ml), and subjected to cell cycle analysis using FACS Canto (Becton Dickinson). Total 30,000 events were analyzed.

Analysis of apoptosis

Cells were processed using an AnnexinV-PI apoptosis assay kit (Life Technologies) and analyzed total 20,000 events by flow cytometry.

Synchronization

HeLa cells were arrested in G0/G1 phase as previously described (16). To arrest in early S phase, double thymidine block method was applied (10). HeLa cells were arrested in M phase as described (17).

Tet-inducible short hairpin RNA constructs

PCTAIRE1 shRNA#1 (GCTCTCATCACTCCTTCACTT), PCTAIRE1 shRNA#2 (GACCTACATTAAGCTGGACAA), and scramble-control (CAACAAGATGAAGAGCACCAA) were cloned into the inducible pLKO-Tet-On vectors as previously described (18).

Yeast two hybrid screening

Library screening by the yeast two hybrid method was performed as described (19) using the pGilda plasmid encoding human PCTAIRE1 as bait, and cDNA libraries derived from human Jurkat T-cells, prostate cancer cell lines (PPC1, Du145, and PC-3), and the EGY48 yeast strain.

Immunofluorescence and conforcal microscopy

Immunofluorescence staining was performed as described (20). Cell imaging was accomplished with a LSM710 NLO Zeiss Conforcal microscope.

Tumor xenograft experiments

All animal experiments were approved by the IACUC of the Sanford-Burnham Medical Research Institute. 5.0×10^6 PPC1 cells resuspended in 200 μl RPMI1640 were injected subcutaneously into the flanks of *nu/nu* mice. Tumor volume was calculated using the following formula: (long axis x short axis^2)/2.

Immunohistochemistry

Dewaxed tissue sections (4.0–5.0 μm) were immunostained as reported previously (21). The information for patient specimens was described in supplementary Materials and Methods.

Quantitative Measurement and Statistical Analysis

Immunoblots band intensities were measured by Image J. Means and standard deviation (SD) were calculated statistically from three determinations. Statistical significance of differences between various samples was determined by Student's t-test. $p < 0.05$ was considered significant.

For additional details, refer to the Supplementary Materials and Methods.

RESULTS

Knockdown of PCTAIRE1 regulates tumor cell growth and proliferation

To investigate the effect of PCTAIRE1 knockdown in cancer cells, we performed siRNA experiments using three siRNAs that target PCTAIRE1 mRNA. Quantitative RT-PCR and immunoblotting confirmed reduction of mRNA and protein levels by all three siRNAs (Supplementary Fig. S1, A and B). Next, prostate cancer PPC1 cells were treated with siRNAs and cell viability was assessed 72 hours later. Cultures of PCTAIRE1 knockdown PPC1 cells showed reduced relative numbers of viable cells compared to control cell cultures (Supplementary Fig. S1C). Similar results were obtained by direct cell counting methods (Supplementary Fig. S1D). Annexin V staining showed increases in cell death over time in cultures of PCTAIRE1 RNAi-treated cells (Supplementary Fig. S1E).

We also used tetracycline-inducible shRNA vectors to assess the impact of PCTAIRE1 deficiency on tumor cells. In PPC1 cells that were stably infected with lentivirus expressing two different shRNAs, culturing with the tetracycline analog doxycycline resulted in concentration-dependent reductions in PCTAIRE1 mRNA levels (Supplementary Fig. S1F). Doxycycline-inducible reductions in PCTAIRE1 protein were also observed (Fig. 1A). In contrast, PCTAIRE1-targeting shRNAs did not reduce levels of mRNAs encoding Cdk1, Cdk2, Cdk4, Cdk5, Cdk6, PCTAIRE2, or PCTAIRE3 (data not shown). Compared to control cells (Tet-OFF), growth rates of doxycycline-stimulated PCTAIRE1 knockdown PPC1 cells (Tet-ON) were significantly diminished 5 days after seeding (Fig. 1B). In clonogenic assays, the number of tumor cell colonies was significantly lower upon PCTAIRE1 knockdown compared to control cells (Fig. 1C). Also, cell death was induced by PCTAIRE1 shRNA expression, as demonstrated by accumulation of annexin V-positive cells (Supplementary Fig. S1G).

To extend these studies into an *in vivo* context, we used PPC1 cells containing inducible shRNA (#2) in a tumor xenograft model. Immunocompromised (*nu/nu*) mice were injected subcutaneously with PPC1 cells, and tumors were allowed to grow for seven days before doxycycline was added to the drinking water for 12 days to induce the shRNA vector, which resulted in reduced PCTAIRE1 protein expression (Supplementary Fig. S1H). Inducing PCTAIRE1 shRNA expression remarkably suppressed tumor growth (Fig. 1, D and E).

Immunohistochemistry analysis showed increased expression of apoptotic markers (TUNEL assay and cleaved-PARP) in resected PCTAIRE1 knockdown tumors (Supplementary Fig. S1I). Similar results were obtained using other tumor cell lines, such as Du145, MDA-MB-468, and HeLa cells (Supplementary Fig. S2). From these results, we conclude that PCTAIRE1 regulates proliferation and survival of cancer cells. However, as expected by the heterogeneity of human cancer, the impact of PCTAIRE1 knockdown was not uniform, in that less robust effects were observed with T47D and MCF7 (data not shown).

Next, we assessed the PCTAIRE1 knockdown effect on normal cells. In the human diploid fibroblast line IMR-90, PCTAIRE1 knockdown did not affect cell growth (Fig. 2, A–C). To further examine the role of PCTAIRE1 in normal versus transformed cells, we applied PCTAIRE1 siRNAs to immortalized prostate epithelial cells 267B1 and their K-ras (V12) transformed isogenic counterpart 267B1/K-ras cells (15). Cell proliferation assays revealed that PCTAIRE1 knockdown markedly diminished the growth rate of 267B1/K-ras cells, whereas the growth of non-transformed 267B1 cells did not appreciably change with PCTAIRE1 knockdown (Fig. 2, D–F). These results suggest that proliferation of transformed cells is preferentially dependent on PCTAIRE1.

PCTAIRE1 plays a role in mitosis in cancer cells

To examine the mechanisms of cell growth suppression caused by PCTAIRE1 knockdown, cell cycle analyses were performed. In cultures of PCTAIRE1 knockdown cells, the proportion of M-phase cells (4N DNA content and phospho-H3 positive) was increased at 24–72 hours, then declined as hypoploid (apoptotic) cells appeared in cultures at 48–96 hours (Fig. 3A). Similar results were obtained for HeLa cells (Supplementary Fig. S3A).

To identify a cell cycle arrest point, we examined the effects of PCTAIRE1 knockdown on cell division using time-lapse video microscopy. Whereas control PPC1 cells (Tet-OFF) completed mitosis in a timely fashion (Supplementary Fig. S3B, top), doxycycline-treated PPC1 cells (Tet-ON) experienced cell division defects. Most of the affected cells arrested in prometaphase for several hours (7.5 ± 1.6 hours, mean ± SD, n = 10), and then underwent an apoptosis (Supplementary Fig. S3B, bottom).

During the prophase to prometaphase transition, duplicated centrosomes migrate to opposite poles (22). To explore the reason for the prometaphase arrest of PCTAIRE1 knockdown cells, we examined in more detail the apparent failure of PCTAIRE1 knockdown PPC1 cells to form bipolar spindles. Prometaphase cells exhibiting failure to separate duplicated centrosomes were two to four times more frequent, and constituted more than 40% of the cells in cultures of PCTAIRE1 knockdown PPC1 cells (Tet-ON), compared with control PPC1 cells (Tet-OFF), (Fig. 3, B and C). Similar phenotypes were observed in siRNA-mediated knockdown of PCTAIRE1 in PPC1 and 267B1/K-ras cells (Fig. 3, D and E, Supplementary Fig. S3, C and D). However, knocking down PCTAIRE1 in 267B1 immortalized prostate epithelial cells did not increase the frequency of cells showing failure to separate duplicated centrosomes (Supplementary Fig. S3, E and F), suggesting that transforming oncoproteins such as K-ras create PCTAIRE1 dependency for centrosome regulation. Altogether, these results suggest that PCTAIRE1 is indispensable for cell division in susceptible cancer cells but not normal cells.

PCTAIRE1 phosphorylates p27 at Ser 10

To identify potential targets of PCTAIRE1, we performed yeast two-hybrid screens of cDNA libraries. From a screen of 15 million initial transformants, 17 were identified that interacted specifically with PCTAIRE1. From this pool of 17 candidate interactors, two were found to encode the tumor suppressor p27. The p27 protein exhibited specific interactions with PCTAIRE1 in two-hybrid assays when tested against other proteins (Fig. 4, A and B, Supplementary Table S1). Interaction of PCTAIRE1 with p27 was confirmed by a co-immunoprecipitation analysis (Supplementary Fig. S4A). Further, immunostaining for both p27 and PCTAIRE1 was observed in both the nucleus and cytoplasm (Fig. 4C). In merged images, co-localization of p27-PCTAIRE1 was observed mainly in nuclei. This result is compatible with PCTAIRE1 localization assessed by subcellular fractionation (Supplementary Fig. S4B). However, we failed to detect interaction of endogenous PCTAIRE1 and p27 by immunoprecipitation assay (data not shown), suggesting that interaction between PCTAIRE1 and p27 is probably transient or weak - which is consistent with the notion that p27 could be a substrate of PCTAIRE1 rather than p27 operating as an inhibitor of PCTAIRE1 akin to its role in binding and suppressing cyclin/Cdk complexes.

It has been reported that p27 is phosphorylated at Ser10, Thr187, and Thr198 (23). To examine whether PCTAIRE1 phosphorylates p27, PPC1 cells were co-transfected with HA-PCTAIRE1 and Myc-p27, followed by immunoprecipitation using anti-Myc antibody, and analysis of specimens by phos-tag SDS-PAGE/immunoblotting. p27 phosphorylation at Ser10 appeared to be remarkably elevated in PCTAIRE1-overexpressing cells (Supplementary Fig. S4C). We also assessed immunoprecipitated proteins using phospho-specific antibodies recognizing p27 phosphorylated at Ser10, Thr187, and Thr198. Again, we found that the levels of p27 phosphorylation at Ser10 were increased in PCTAIRE1-overexpressing cells (Supplementary Fig. S4D and data not shown). Conversely, levels of p27 Ser10 phosphorylation were reduced in PPC1 cells with PCTAIRE1 knockdown (Supplementary Fig. S4, E and F). By subcellular fractionation, shRNA-knockdown (Tet-ON) resulted in lower levels of endogenous p27 (Ser10) phosphorylation in nuclei compared to control cells (Tet-OFF) (Fig. 4D).

Finally, we used an *in vitro* kinase assay to assess PCTAIRE1 phosphorylation of p27, employing purified p27 as substrate and immunoprecipitated PCTAIRE1 as enzyme, thereby confirming that PCTAIRE1 can directly phosphorylate p27 at Ser10 (Supplementary Fig. S4G). In contrast, a kinase-dead PCTAIRE1 mutant (K194M), PCTAIRE2, and PCTAIRE3 did not phosphorylate p27 (Supplementary Fig. S4, G and H). PCTAIRE1 phosphorylation of p27 was inhibited by the pan-Cdk inhibitor SNS-032 (Supplementary Fig. S4I).

PCTAIRE1 knockdown leads to p27 accumulation

The levels of p27 are regulated by phosphorylation-induced ubiquitination/degradation (Supplementary Fig. S5A), with phosphorylation at Ser10 playing a critical role (14, 23, 24). PCTAIRE1 knockdown up-regulated p27 protein levels in PPC1 cells (Fig. 5, A and B, Supplementary Fig. S5B), while p27 mRNA levels were unaffected (Supplementary Fig. S5, C and D). Elevated levels of p27 protein were also observed in PCTAIRE1 knockdown tumor xenografts (Fig. 5C). In contrast, knockdown of Cdk1 or Cdk5 showed no effect on

p27 protein levels (Supplementary Fig. S5, E and F). Up-regulation of p27 protein levels by PCTAIRE1 knockdown was also seen for other tumor cell lines, including MDA-MB-468, Du145, and 267B1/K-ras cells (Supplementary Fig. S5, G, H, I, and N). Meanwhile, PCTAIRE1 knockdown did not induce p27 up-regulation in T47D, MCF7, IMR-90, or 267B1 cells (Supplementary Fig. S5, J–O), correlating with the lack of PCTAIRE1 dependence for growth of these cell lines.

As a complement to RNAi experiments, we assessed the impact of PCTAIRE1 overexpression on p27 protein levels using 267B1 cells, which intrinsically contain low PCTAIRE1. Experimentally overexpressing PCTAIRE1 in these cells caused p27 Ser10 phosphorylation (Supplementary Fig. S5P), and reduced p27 protein levels in a proteasome-dependent manner (Supplementary Fig. S5Q). In contrast, expressing kinase dead PCTAIRE1 mutant failed to modulate p27.

The effect of PCTAIRE1 on p27 protein stability was further examined by cyclohexamide (CHX) chase experiments. PPC1 cells with shRNA (#2) were cultured with (ON) or without (OFF) doxycycline for 48 hours whereupon the cells were treated with 25 μg/ml cyclohexamide and the rate of p27 turnover was monitored (Fig. 5D). Endogenous p27 protein levels were significantly more stable in PCTAIRE1 knockdown PPC1 cells than in control PPC1 cells, demonstrating that PCTAIRE1 down-regulates p27 in a post-translational manner. Furthermore, based on subcellular fractionation analysis, we determined that PCTAIRE1 knockdown appears to promote p27 accumulation in both nucleus and cytoplasm (Fig. 5E).

Next, we examined the cell cycle dependence of p27 (Ser10) phosphorylation, p27 accumulation, and mitotic arrest in the context of PCTAIRE1 knockdown. For these experiments, we used HeLa cells in which PCTAIRE1 knockdown upregulates p27 protein (Fig. 6, A and B). We used a cell synchronization method to assess regulation of p27 levels, employing release from double thymidine block (Supplementary Fig. S6A). The levels of p27 protein in Tet-OFF HeLa cells gradually declined following release from cell cycle arrest, whereas p27 levels in Tet-ON cells were continuously elevated until M phase, when apoptosis occurred as indicated by cleavage of caspase-3 (Fig. 6C). The cell cycle-dependent cleavage of caspase-3 during M-phase in PCTAIRE1-deficient cells was independently confirmed by other cell cycle synchronization procedures (Supplementary Fig. S6B). Finally, we examined whether the phosphorylation of p27 (Ser10) by PCTAIRE1 is dependent on phase of the cell cycle. Phos-tag SDS-PAGE/immunoblot analysis revealed that PCTAIRE1 knockdown modulates p27 phosphorylation (Ser10) during S-M phases (Fig. 6D), which is consistent with a previous study (10).

To investigate the pathogenic mechanism of defective mitosis caused by PCTAIRE1 knockdown in susceptible cancer cell lines, we assessed expression of critical proteins required for centrosome separation: Cdk1, Cdk2, cyclin B1, and Eg5 (25, 26). In PCTAIRE1 knockdown cells, protein expression of these molecules was normal (Supplementary Fig. S6, C and D). Next, we assessed the impact of PCTAIRE1 on interaction of p27 with Cdks that it is known to bind and suppress. The p27 protein that accumulated in PCTAIRE1 knockdown cells was found to interact with Cdk1 and Cdk2 (Supplementary Fig. S6E),

suggesting that p27 retains its ability to suppress target Cdks. Cdk1 and Cdk2 are indispensable molecules in centrosome separation because these Cdks regulate centrosome localization of Eg5 (27, 28). We determined Eg5 localization during late G2-prometaphase by immunofluorescence microscopy. While Eg5 co-localized with centrosomes in control cells, Eg5 failed to associate with centrosomes during late G2-prophase in PCTAIRE1 knockdown cells (Supplementary Fig. S6, F and G).

To confirm the functional role of p27 in the aberrant centrosome dynamics caused by PCTAIRE1 knockdown, PPC1 cells were transfected with siRNAs targeting PCTAIRE1, p27, or both, as well as with various control synthetic RNAs (Fig. 6E). We found that p27 knockdown partially rescued cell viability in cultures of PCTAIRE1 knockdown PPC1 cells (Fig. 6F). Knockdown of p27 also substantially improved growth of PCTAIRE1 knockdown cells (Fig. 6G). Furthermore, the frequency of unseparated duplicated centrosomes was decreased in p27/PCTAIRE1 double knockdown compared to PCTAIRE1-single knockdown cells (Fig. 6H).

Elevated levels of PCTAIRE1 in malignant tissues

We assessed the status of PCTAIRE1 expression in primary prostate and breast tumor specimens by immunohistochemistry using tissue microarrays (TMAs). To characterize the specificity of the anti-PCTAIRE1 antibody, immunoblot analysis was performed (Supplementary Fig. S7, A–C). PCTAIRE1 immunostaining was very low in normal prostate glands (Fig. 7, A, B, and C), but markedly higher in both prostatic intraepithelial neoplasia (PIN) and invasive cancers (Fig. 7, A and C). Comparison of PCTAIRE1 immunostaining with Gleason grade revealed low expression levels in very well-differentiated tumors (Gleason grade 2) compared to less differentiated tumors (Gleason grades 3–5) (Fig. 7D).

For breast cancer analyses, TMAs containing tumor specimens derived from 121 patients were immunostained. PCTAIRE1 expression was significantly elevated in *in situ* carcinomas and invasive cancers compared to normal mammary epithelium (Fig. 7, E–G). Significantly higher levels of PCTAIRE1 protein in invasive cancers were associated with increasing histologic grade (Fig. 7H), more advanced stage of disease (Fig. 7I), and negative immunostaining for progesterone receptor (PR) (Fig. 7J). In this specimen collection, no correlations were found between PCTAIRE1 protein expression and tumor size, estrogen receptor-α status, or survival. Based on the immunohistochemical pattern of staining, the localization of PCTAIRE1 in primary tumors appeared to include both nuclei and cytoplasm (Supplementary Fig. S7D).

We further examined the expression of p27 in the prostate TMA samples, which showed that PCTAIRE1 and p27 levels were inversely correlated (Supplementary Fig. S7, E and F). These findings are consistent with our cell culture results showing that knockdown of PCTAIRE1 stabilizes p27.

Next, we assessed PCTAIRE1 and p27 protein expression levels in various cell lines. Compared to normal cell lines (IMR-90 and 267B1 cells), tumor cell lines (PPC1, Du145, 267B1/K-ras, HeLa, and MDA-MB-468, which are sensitive to PCTAIRE1 knockdown)

showed higher PCTAIRE1and lower p27 protein levels (Supplementary Fig. S7G). In breast cancer MCF7 and T47D cells, which are not sensitive to PCTAIRE1 knockdown, p27 expression levels were higher compared to other cancer cells. These results suggest that baseline expression levels of p27 and PCTAIRE1 may differentiate PCTAIRE1-dependent from -independent malignancies.

We also assessed PCTAIRE1 protein isoforms based on the evidence for diverse PCTAIRE1 isoforms in mouse tissues (6). Compared to PCTAIRE1-knockdown cell lysates (employed as negative controls), only one band was detected for human PCTAIRE1 (Supplementary Fig. S7H), suggesting the presence of only one major isoform of PCTAIRE1 in the human cell lines we assessed.

To further assess the role of PCTAIRE1 in cancers, we used the Oncomine data base to evaluate the levels of *PCTAIRE1* expression. When 15 studies containing informative *PCATIRE1* expression levels were combined, *PCTAIRE1* was identified as one of the most upregulated genes in cancers compared with corresponding normal tissues (Supplementary Fig. S8A). Further, several studies showed evidence of PCTAIRE1 copy number gains in cancers (Supplementary Fig. S8B), which suggests that gene amplification may be one of the reasons for *PCTAIRE1* overexpression. Finally, the prognostic value of *PCTAIRE1* was assessed using Kaplan-Meier Plotter, an online tool to correlate survival with gene expression, based upon microarray data from 1,405 patients with lung cancer and 1,115 patients with breast cancer. High *PCTAIRE1* mRNA levels were significantly correlated with lower overall survival in lung (Supplementary Fig. S8C) and breast cancers (Supplementary Fig. S8D).

Discussion

We report here an unexpected role for PCTAIRE1 in cancer cell division (Fig. 7K). In normal tissues, PCTAIRE1 is highly expressed in testis and brain (2). A physiological function for PCTAIRE1 was discovered in neurons of PCT-1 mutant nematodes (29), while PCTAIRE1 was implicated by gene ablation studies in mice to be involved in spermatogenesis (6). Analysis of PCTAIRE1 knock-out mice revealed no essential requirement of PCTAIRE1 for cell proliferation in normal tissues, since PCTAIRE1-deficient mice are viable (6). Consistent with these reports, we also did not detect a role for PCTAIRE1 in proliferation of non-transformed cells. Rather, the participation of PCTAIRE1 in cell division was evident in certain cancerous cells.

Our study identified the tumor suppressor p27 as a novel substrate of PCTAIRE1. The importance of p27 as a negative regulator of cell proliferation is illustrated by the phenotype of $p27^{-/-}$ mice, which exhibit increased body size and are predisposed to tumorigenesis (30–33). The main phosphorylation site on p27 is Ser10, which has been found to regulate both its subcellular localization and stability (34, 35). Interestingly, Ser10 phosphorylation can be associated with either stabilization or degradation of p27, depending on the cell cycle. For example, phosphorylation at this site, or mutation of Ser10 to a phospho-mimetic residue (Asp or Glu), correlates with increased stability of p27 in non-dividing cells (34–37). In contrast, Ser10 phosphorylation has also been linked to p27 degradation in cycling cells.

Several groups reported that p27 Ser10 phosphorylation was required for its export from the nucleus (34–36, 38–40), which may trigger p27 degradation (24). Phosphorylation of Ser10 has additionally been suggested to be involved in a cancer-related p27 degradation pathway. Phosphorylation-resistant p27-S10A-knock-in mice are partially resistant to urethane-induced tumorigenesis (41). Thus, phosphorylation of Ser10 may constitute an important pathway by which tumor cells modulate the tumor suppressor function of p27.

Several kinases are capable of phosphorylating p27 at Ser10. For example, Mirk/Dyrk1B phosphorylates and stabilizes p27 in quiescent cells (37), while hKIS phosphorylates this site at the G0–G1 phase transition following mitogen stimulation, which is accompanied by translocation of p27 (36). Cdk5 also phosphorylates p27 at Ser10 and promotes neural migration in the developing cerebral cortex (42). Other kinases, such as PKB/Akt and ERK2, were reported to phosphorylate p27 at Ser10 (34, 43). These various protein kinases may be capable of modulating the tumor suppressor function of p27, implying considerable redundancy in the mechanisms that promote malignant cell growth via p27 dysregulation. In this regard, while PCTAIRE1 knockdown caused mitotic defects in PPC1, Du145, MDA-MB-468, HeLa, and 267B1/K-ras cells, we observed no remarkable reduction in cell proliferation or survival upon PCTAIRE1 knockdown in the T47D and MCF7 cells. Thus, the role of PCTAIRE1 in p27 dysregulation is likely to be heterogeneous among cancers, and further analysis will be required to differentiate PCTAIRE1-dependent from -independent malignancies.

Our study also suggested a novel role for PCTAIRE1 and p27 in the regulation of centrosome dynamics. While the role of p27 in the late phase of the cell cycle is unclear, several studies indicated that p27 participates in mitosis. Knockout of Skp2 leads to impaired degradation of p27 (44). In *Skp2* knock-out mice, several tissues display an increase in cell size, DNA content, and proliferation defects (44–46). These phenotypes are rescued in double *Skp2*$^{-/-}$ *p27*$^{-/-}$ mice, suggesting that the accumulation of p27 in *Skp2*$^{-/-}$ cells is responsible for the failure to progress through mitosis (45, 46). Though the underlying mechanism is unknown by which aberrant p27 expression causes perturbations in centrosome dynamics, we detected a defect in Eg5 localization to centrosomes in dividing cells, consistent with previous studies (27, 28), suggesting that accumulated p27 may affect centrosome dynamics via a Cdk1/Cdk2-Eg5 pathway.

In summary, inhibition of PCTAIRE1 in tumors containing pathological elevation of this kinase may provide a strategy for improved treatments of some forms of human cancer. In this context, PCTAIRE1 inhibitors would be predicted to restore expression of tumor suppressor p27, reestablishing a mechanism that interferes with prometaphase to metaphase transition (presumably by altering centrosome dynamics) and thereby causing apoptosis to circumvent the propagation of malignant cells. Furthermore, the contribution of p27 to prometaphase-metaphase arrest is presumably only relevant to certain transformed cells possessing defects in cell cycle check point regulation.

Supplementary Material

Refer to Web version on PubMed Central for supplementary material.

Acknowledgments

References

1. Cole AR. PCTK proteins: the forgotten brain kinases? Neurosignals. 2009; 17:288–97. [PubMed: 19816065]

2. Le Bouffant F, Le Minter P, Traiffort E, Ruat M, Sladeczek F. Multiple subcellular localizations of PCTAIRE-1 in brain. Mol Cell Neurosci. 2000; 16:388–95. [PubMed: 11085876]

3. Liu Y, Cheng K, Gong K, Fu AK, Ip NY. Pctaire1 phosphorylates N-ethylmaleimide-sensitive fusion protein: implications in the regulation of its hexamerization and exocytosis. J Biol Chem. 2006; 281:9852–8. [PubMed: 16461345]

4. Mokalled MH, Johnson A, Kim Y, Oh J, Olson EN. Myocardin-related transcription factors regulate the Cdk5/Pctaire1 kinase cascade to control neurite outgrowth, neuronal migration and brain development. Development. 2010; 137:2365–74. [PubMed: 20534669]

5. Palmer KJ, Konkel JE, Stephens DJ. PCTAIRE protein kinases interact directly with the COPII complex and modulate secretory cargo transport. J Cell Sci. 2005; 118:3839–47. [PubMed: 16091426]

6. Mikolcevic P, Sigl R, Rauch V, Hess MW, Pfaller K, Barisic M, et al. Cyclin-dependent kinase 16/PCTAIRE kinase 1 is activated by cyclin Y and is essential for spermatogenesis. Mol Cell Biol. 2012; 32:868–79. [PubMed: 22184064]

7. Mikolcevic P, Rainer J, Geley S. Orphan kinases turn eccentric: a new class of cyclin Y-activated, membrane-targeted CDKs. Cell Cycle. 2012; 11:3758–68. [PubMed: 22895054]

8. Graeser R, Gannon J, Poon RY, Dubois T, Aitken A, Hunt T. Regulation of the CDK-related protein kinase PCTAIRE-1 and its possible role in neurite outgrowth in Neuro-2A cells. J Cell Sci. 2002; 115:3479–90. [PubMed: 12154078]

9. Cheng K, Li Z, Fu WY, Wang JH, Fu AK, Ip NY. Pctaire1 interacts with p35 and is a novel substrate for Cdk5/p35. J Biol Chem. 2002; 277:31988–93. [PubMed: 12084709]

10. Charrasse S, Carena I, Hagmann J, Woods-Cook K, Ferrari S. PCTAIRE-1: characterization, subcellular distribution, and cell cycle-dependent kinase activity. Cell Growth Differ. 1999; 10:611–20. [PubMed: 10511311]

11. Chu IM, Hengst L, Slingerland JM. The Cdk inhibitor p27 in human cancer: prognostic potential and relevance to anticancer therapy. Nat Rev Cancer. 2008; 8:253–67. [PubMed: 18354415]

12. Porter PL, Malone KE, Heagerty PJ, Alexander GM, Gatti LA, Firpo EJ, et al. Expression of cell-cycle regulators p27Kip1 and cyclin E, alone and in combination, correlate with survival in young breast cancer patients. Nat Med. 1997; 3:222–5. [PubMed: 9018243]

13. Besson A, Dowdy SF, Roberts JM. CDK inhibitors: cell cycle regulators and beyond. Dev Cell. 2008; 14:159–69. [PubMed: 18267085]

14. Nagano Y, Fukushima T, Okemoto K, Tanaka K, Bowtell DD, Ronai Z, et al. Siah1/SIP regulates p27(kip1) stability and cell migration under metabolic stress. Cell Cycle. 2011; 10:2592–602. [PubMed: 21734459]

15. Parda DS, Thraves PJ, Kuettel MR, Lee MS, Arnstein P, Kaighn ME, et al. Neoplastic transformation of a human prostate epithelial cell line by the v-Ki-ras oncogene. Prostate. 1993; 23:91–8. [PubMed: 8378190]

16. Ishida N, Kitagawa M, Hatakeyama S, Nakayama K. Phosphorylation at serine 10, a major phosphorylation site of p27(Kip1), increases its protein stability. J Biol Chem. 2000; 275:25146–54. [PubMed: 10831586]

17. Yuan J, Kramer A, Matthess Y, Yan R, Spankuch B, Gatje R, et al. Stable gene silencing of cyclin B1 in tumor cells increases susceptibility to taxol and leads to growth arrest in vivo. Oncogene. 2006; 25:1753–62. [PubMed: 16278675]

18. Wiederschain D, Wee S, Chen L, Loo A, Yang G, Huang A, et al. Single-vector inducible lentiviral RNAi system for oncology target validation. Cell Cycle. 2009; 8:498–504. [PubMed: 19177017]

19. Matsuzawa S, Reed JC. Yeast and mammalian two-hybrid systems for studying protein-protein interactions. Methods Mol Biol. 2007; 383:215–25. [PubMed: 18217688]

20. Fujii R, Zhu C, Wen Y, Marusawa H, Bailly-Maitre B, Matsuzawa S, et al. HBXIP, cellular target of hepatitis B virus oncoprotein, is a regulator of centrosome dynamics and cytokinesis. Cancer Res. 2006; 66:9099–107. [PubMed: 16982752]

21. Krajewska M, Smith LH, Rong J, Huang X, Hyer ML, Zeps N, et al. Image analysis algorithms for immunohistochemical assessment of cell death events and fibrosis in tissue sections. J Histochem Cytochem. 2009; 57:649–63. [PubMed: 19289554]

22. Nigg EA. Centrosome aberrations: cause or consequence of cancer progression? Nat Rev Cancer. 2002; 2:815–25. [PubMed: 12415252]

23. Lu Z, Hunter T. Ubiquitylation and proteasomal degradation of the p21(Cip1), p27(Kip1) and p57(Kip2) CDK inhibitors. Cell Cycle. 2010; 9:2342–52. [PubMed: 20519948]

24. Kamura T, Hara T, Matsumoto M, Ishida N, Okumura F, Hatakeyama S, et al. Cytoplasmic ubiquitin ligase KPC regulates proteolysis of p27(Kip1) at G1 phase. Nat Cell Biol. 2004; 6:1229–35. [PubMed: 15531880]

25. Crasta K, Huang P, Morgan G, Winey M, Surana U. Cdk1 regulates centrosome separation by restraining proteolysis of microtubule-associated proteins. EMBO J. 2006; 25:2551–63. [PubMed: 16688214]

26. Lindqvist A, van Zon W, Karlsson Rosenthal C, Wolthuis RM. Cyclin B1-Cdk1 activation continues after centrosome separation to control mitotic progression. PLoS Biol. 2007; 5:e123. [PubMed: 17472438]

27. Blangy A, Lane HA, d'Herin P, Harper M, Kress M, Nigg EA. Phosphorylation by p34cdc2 regulates spindle association of human Eg5, a kinesin-related motor essential for bipolar spindle formation in vivo. Cell. 1995; 83:1159–69. [PubMed: 8548803]

28. Smith E, Hegarat N, Vesely C, Roseboom I, Larch C, Streicher H, et al. Differential control of Eg5-dependent centrosome separation by Plk1 and Cdk1. EMBO J. 2011; 30:2233–45. [PubMed: 21522128]

29. Ou CY, Poon VY, Maeder CI, Watanabe S, Lehrman EK, Fu AK, et al. Two cyclin-dependent kinase pathways are essential for polarized trafficking of presynaptic components. Cell. 2010; 141:846–58. [PubMed: 20510931]

30. Fero ML, Rivkin M, Tasch M, Porter P, Carow CE, Firpo E, et al. A syndrome of multiorgan hyperplasia with features of gigantism, tumorigenesis, and female sterility in p27(Kip1)-deficient mice. Cell. 1996; 85:733–44. [PubMed: 8646781]

31. Kiyokawa H, Kineman RD, Manova-Todorova KO, Soares VC, Hoffman ES, Ono M, et al. Enhanced growth of mice lacking the cyclin-dependent kinase inhibitor function of p27(Kip1). Cell. 1996; 85:721–32. [PubMed: 8646780]

32. Nakayama K, Ishida N, Shirane M, Inomata A, Inoue T, Shishido N, et al. Mice lacking p27(Kip1) display increased body size, multiple organ hyperplasia, retinal dysplasia, and pituitary tumors. Cell. 1996; 85:707–20. [PubMed: 8646779]

33. Fero ML, Randel E, Gurley KE, Roberts JM, Kemp CJ. The murine gene p27Kip1 is haplo-insufficient for tumour suppression. Nature. 1998; 396:177–80. [PubMed: 9823898]

34. Ishida N, Hara T, Kamura T, Yoshida M, Nakayama K, Nakayama KI. Phosphorylation of p27Kip1 on serine 10 is required for its binding to CRM1 and nuclear export. J Biol Chem. 2002; 277:14355–8. [PubMed: 11889117]

35. Rodier G, Montagnoli A, Di Marcotullio L, Coulombe P, Draetta GF, Pagano M, et al. p27 cytoplasmic localization is regulated by phosphorylation on Ser10 and is not a prerequisite for its proteolysis. EMBO J. 2001; 20:6672–82. [PubMed: 11726503]

36. Boehm M, Yoshimoto T, Crook MF, Nallamshetty S, True A, Nabel GJ, et al. A growth factor-dependent nuclear kinase phosphorylates p27(Kip1) and regulates cell cycle progression. EMBO J. 2002; 21:3390–401. [PubMed: 12093740]

37. Deng X, Mercer SE, Shah S, Ewton DZ, Friedman E. The cyclin-dependent kinase inhibitor p27Kip1 is stabilized in G(0) by Mirk/dyrk1B kinase. J Biol Chem. 2004; 279:22498–504. [PubMed: 15010468]

38. Connor MK, Kotchetkov R, Cariou S, Resch A, Lupetti R, Beniston RG, et al. CRM1/Ran-mediated nuclear export of p27(Kip1) involves a nuclear export signal and links p27 export and proteolysis. Mol Biol Cell. 2003; 14:201–13. [PubMed: 12529437]

39. McAllister SS, Becker-Hapak M, Pintucci G, Pagano M, Dowdy SF. Novel p27(kip1) C-terminal scatter domain mediates Rac-dependent cell migration independent of cell cycle arrest functions. Mol Cell Biol. 2003; 23:216–28. [PubMed: 12482975]

40. Shin I, Rotty J, Wu FY, Arteaga CL. Phosphorylation of p27Kip1 at Thr-157 interferes with its association with importin alpha during G1 and prevents nuclear re-entry. J Biol Chem. 2005; 280:6055–63. [PubMed: 15579463]

41. Besson A, Gurian-West M, Chen X, Kelly-Spratt KS, Kemp CJ, Roberts JM. A pathway in quiescent cells that controls p27Kip1 stability, subcellular localization, and tumor suppression. Genes Dev. 2006; 20:47–64. [PubMed: 16391232]

42. Kawauchi T, Chihama K, Nabeshima Y, Hoshino M. Cdk5 phosphorylates and stabilizes p27kip1 contributing to actin organization and cortical neuronal migration. Nat Cell Biol. 2006; 8:17–26. [PubMed: 16341208]

43. Fujita N, Sato S, Katayama K, Tsuruo T. Akt-dependent phosphorylation of p27Kip1 promotes binding to 14-3-3 and cytoplasmic localization. J Biol Chem. 2002; 277:28706–13. [PubMed: 12042314]

44. Nakayama K, Nagahama H, Minamishima YA, Matsumoto M, Nakamichi I, Kitagawa K, et al. Targeted disruption of Skp2 results in accumulation of cyclin E and p27(Kip1), polyploidy and centrosome overduplication. EMBO J. 2000; 19:2069–81. [PubMed: 10790373]

45. Nakayama K, Nagahama H, Minamishima YA, Miyake S, Ishida N, Hatakeyama S, et al. Skp2-mediated degradation of p27 regulates progression into mitosis. Dev Cell. 2004; 6:661–72. [PubMed: 15130491]

46. Kossatz U, Dietrich N, Zender L, Buer J, Manns MP, Malek NP. Skp2-dependent degradation of p27kip1 is essential for cell cycle progression. Genes Dev. 2004; 18:2602–7. [PubMed: 15520280]
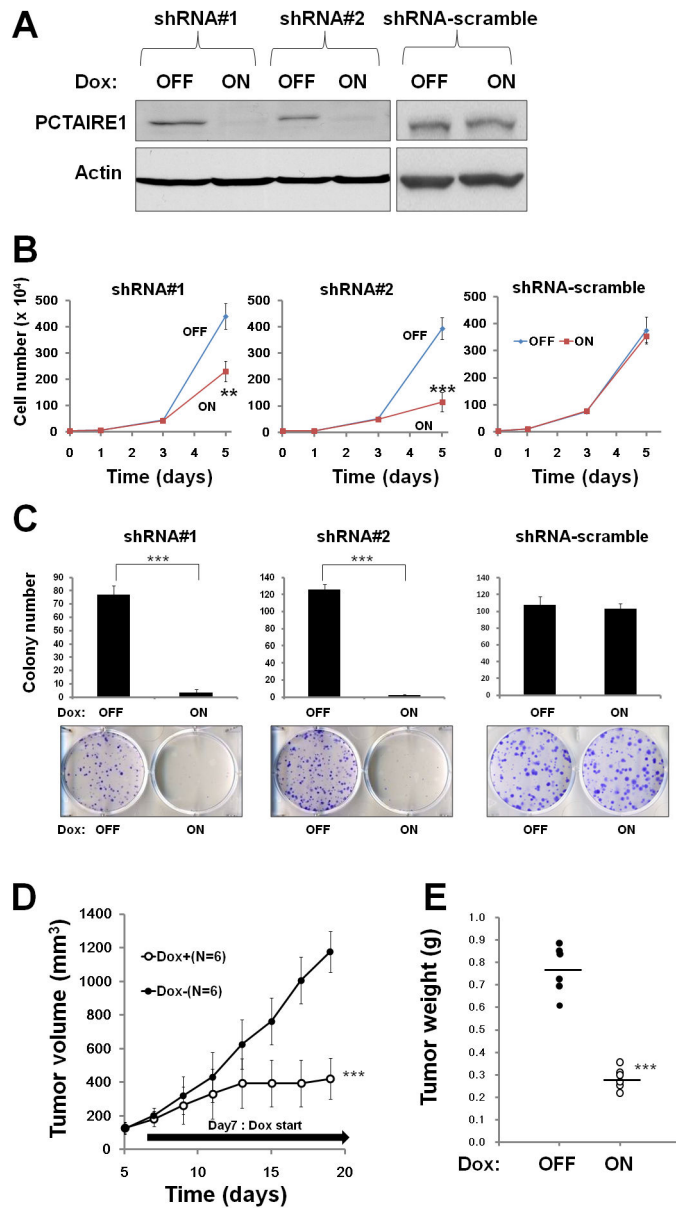
Fig. 1. Knockdown of PCTAIRE1 diminishes PPC1 cell growth

(A) Protein lysates were generated from PPC1 cells stably containing inducible shRNAs (#1, #2) and scramble control cultured for 48 hours with or without 100 ng/ml doxycycline, and analyzed by immunoblotting.

(B) PPC1 cells (5.0×10^4) stably containing shRNAs were cultured for 24 hours, then stimulated with (ON) or without (OFF) doxycycline. The numbers of cells were counted (mean ± SD; n = 3). ** $p < 0.01$, *** $p < 0.001$

(C) PPC1 cells with inducible shRNAs were seeded at 300 cells per well. After 24 hours, doxycycline was added. Colonies consisting of > 50 cells were enumerated on day 10. All data represent mean ± SD (n = 3). *** $p < 0.001$
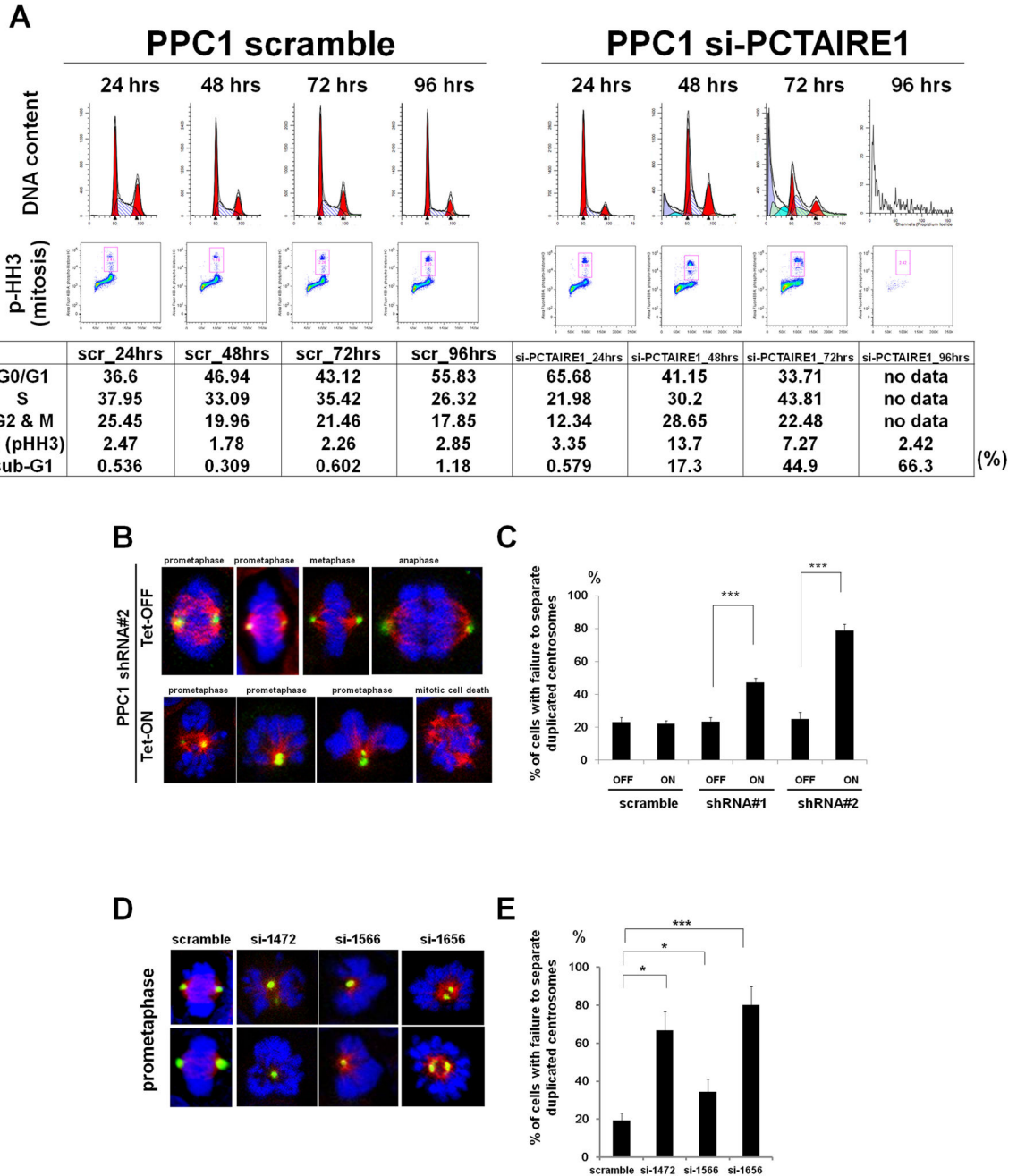
(D) PPC1 cells (shRNA#2) were subcutaneously injected into *nu/nu* mice. When tumor volumes reached 150–200 mm^3, the animals were provided water with (white circles) or without (black circles) 2% doxycycline ("Dox") (mean ± SD). *** p < 0.001

(E) Tumors recovered from sacrificed mice at day 19 were weighed (mean = horizontal line). *** p < 0.001
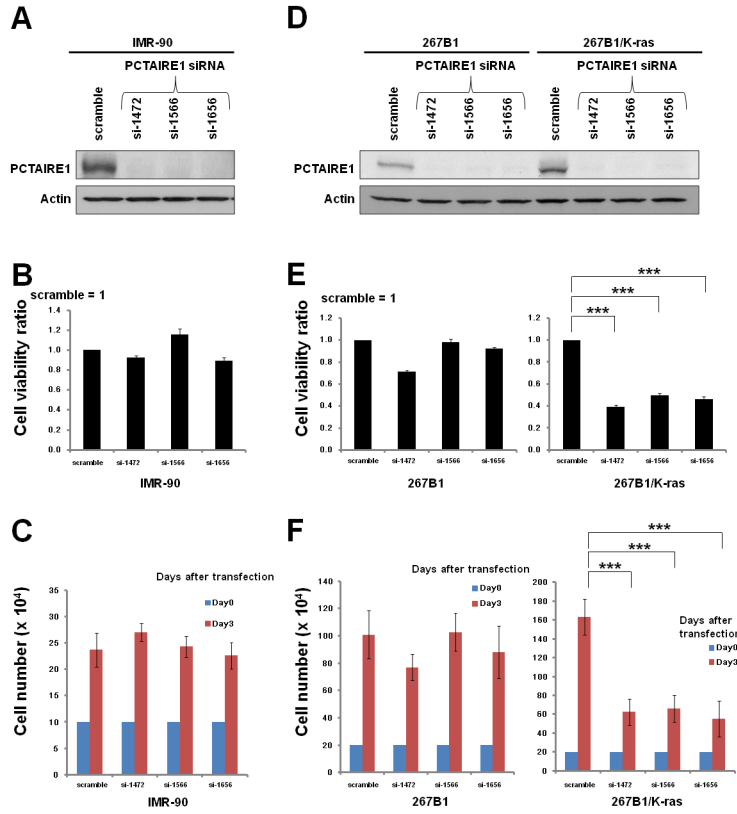
Fig. 2. Transformed cells are preferentially dependent on PCTAIRE1 for proliferation

(A, D) IMR-90, 267B1 and K-ras transformed 267B1 (267B1/K-ras) cells were transfected with siRNAs as indicated. At 3 days after transfection, cell lysates were analyzed by immunoblotting.

(B, E) 72 hours after siRNA transfection, cellular ATP levels were measured (mean ± SD; n = 3). *** p< 0.001

(C, F) To measure cell growth, 2.0×10^5 cells transfected with the indicated siRNAs were plated. After 72 hours, the number of cells was counted (mean ± SD; n = 3). *** p < 0.001

A

PPC1 scramble | **PPC1 si-PCTAIRE1**

DNA content

24 hrs | 48 hrs | 72 hrs | 96 hrs | 24 hrs | 48 hrs | 72 hrs | 96 hrs

p-HH3 (mitosis)

	scr_24hrs	scr_48hrs	scr_72hrs	scr_96hrs	si-PCTAIRE1_24hrs	si-PCTAIRE1_48hrs	si-PCTAIRE1_72hrs	si-PCTAIRE1_96hrs
G0/G1	36.6	46.94	43.12	55.83	65.68	41.15	33.71	no data
S	37.95	33.09	35.42	26.32	21.98	30.2	43.81	no data
G2 & M	25.45	19.96	21.46	17.85	12.34	28.65	22.48	no data
M (pHH3)	2.47	1.78	2.26	2.85	3.35	13.7	7.27	2.42
sub-G1	0.536	0.309	0.602	1.18	0.579	17.3	44.9	66.3

(%)

B

PPC1 shRNA#2

Tet-OFF: prometaphase | prometaphase | metaphase | anaphase

Tet-ON: prometaphase | prometaphase | prometaphase | mitotic cell death

C

% of cells with failure to separate duplicated centrosomes

*** ***

OFF ON OFF ON OFF ON
scramble | shRNA#1 | shRNA#2

D

prometaphase

scramble | si-1472 | si-1566 | si-1656

E

% of cells with failure to separate duplicated centrosomes

*** * *

scramble si-1472 si-1566 si-1656

Fig. 3. PCTAIRE1 regulates centrosome dynamics

(A) PPC1 cells transfected with siRNAs (scramble or si-PCTAIRE1-1656) were cultured for various times as indicated, followed by FACS analysis. Data in upper panels represent relative DNA versus relative cell number. Data in lower panels represent DNA content versus phospho-H3 immunostaining. Red boxes indicate mitotic cells.

(B, C) PPC1 cells stably containing inducible shRNAs were cultured with (Tet-ON) or without (Tet-OFF) 100 ng/ml doxycycline, then fixed and stained using antibodies for pericentrin (green), or alpha-tubulin (red), followed by DAPI (blue). (B) Representative photographs of cells stimulated with or without doxycycline. (C) The percentage of cells

with failure to separate duplicated centrosomes among prometaphase cells was enumerated. *Columns*, mean (n = 3, determinations based on examination of 100 prometaphase cells); *bar*, SD. *** p< 0.001

(D, E) PPC1 cells were transfected with siRNAs, then fixed and stained 2 days later. (D) Representative photographs are shown. (E) The percentage of cells with failure to separate duplicated centrosomes was enumerated (mean ± SD; n = 3). * p < 0.05, *** p < 0.001
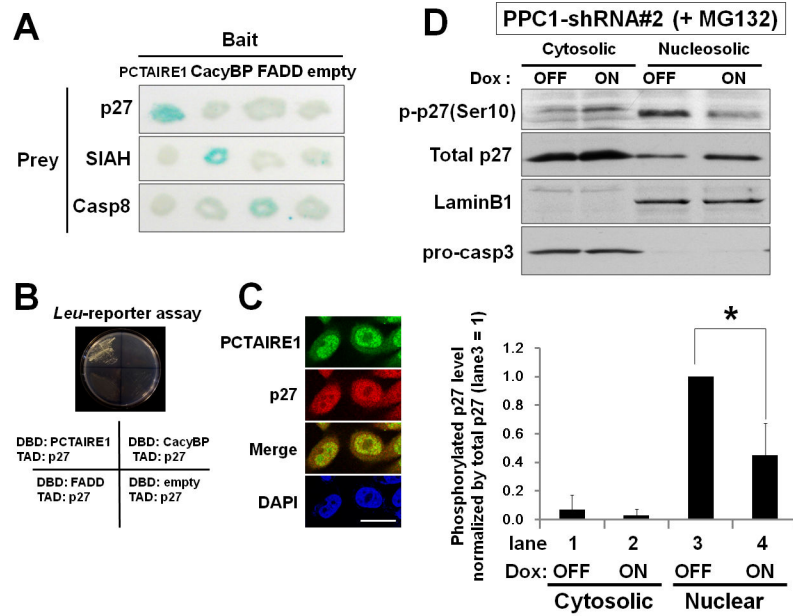
Fig. 4. PCTAIRE1 phosphorylates p27 at Ser 10

(A, B) The specificity of two-hybrid interactions was evaluated by yeast transformed with plasmids that contained different bait plasmids encoding the various LexA DNA-binding domain (DBD) fusion proteins (PCTAIRE1, Calcyclin binding protein (CacyBP), FADD, or empty) and different prey plasmids encoding various B42 transactivation domain (TAD) fusion proteins (p27, SIAH1, Caspase-8). (A) Beta-galactosidase activity of each colony was tested by filter assay and scored as blue (+) or white (–) after 90 minutes. (B) Interactions were detected by transactivation of *LEU2* reporter genes. Growth on leucine-deficient medium at 30 °C was examined 4 days later.

(C) PPC1 cells were immunostained with anti-PCTAIRE1 (green) and anti-p27 (red) antibodies and DNA-binding fluorochrome DAPI (blue). Scale bar = 20 μm.

(D) (Top) PPC1 cells stably containing inducible shRNA targeting PCTAIRE1 (shRNA#2) were cultured with (ON) or without (OFF) 100 ng/ml doxycycline (Dox). After 48 hours, cells were treated with MG132 (10 μM) for 4 hours. Cells were fractionated to yield cytosolic and nuclear compartments. (Bottom) The expression level of phosphorylated p27 (Ser10) was quantified and normalized relative to total p27. Data were expressed relative to phosphorylated p27 (Ser10) in lane 3 (nuclear fraction without PCTAIRE1 knockdown). * p < 0.05
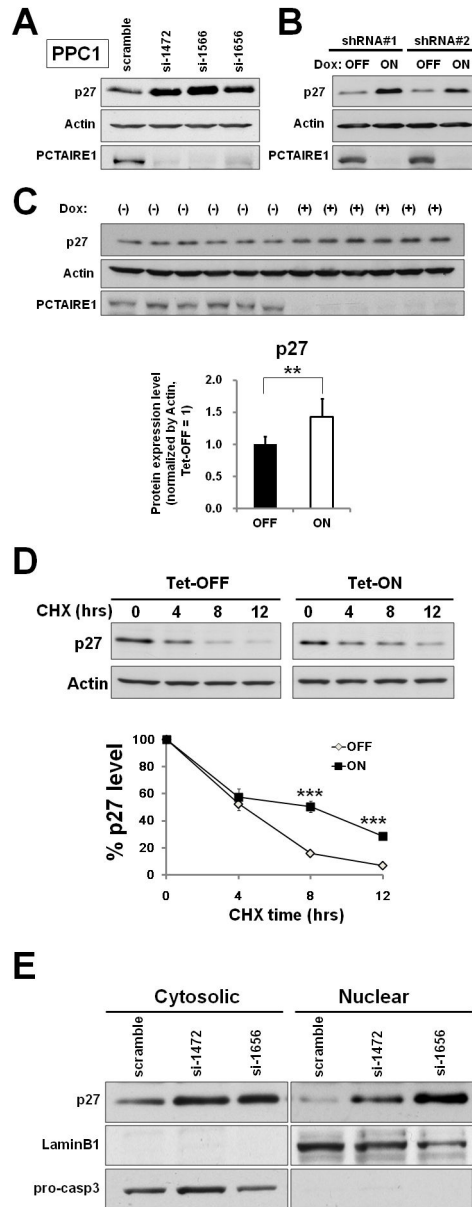
Fig. 5. PCTAIRE1 knockdown leads to accumulation of p27

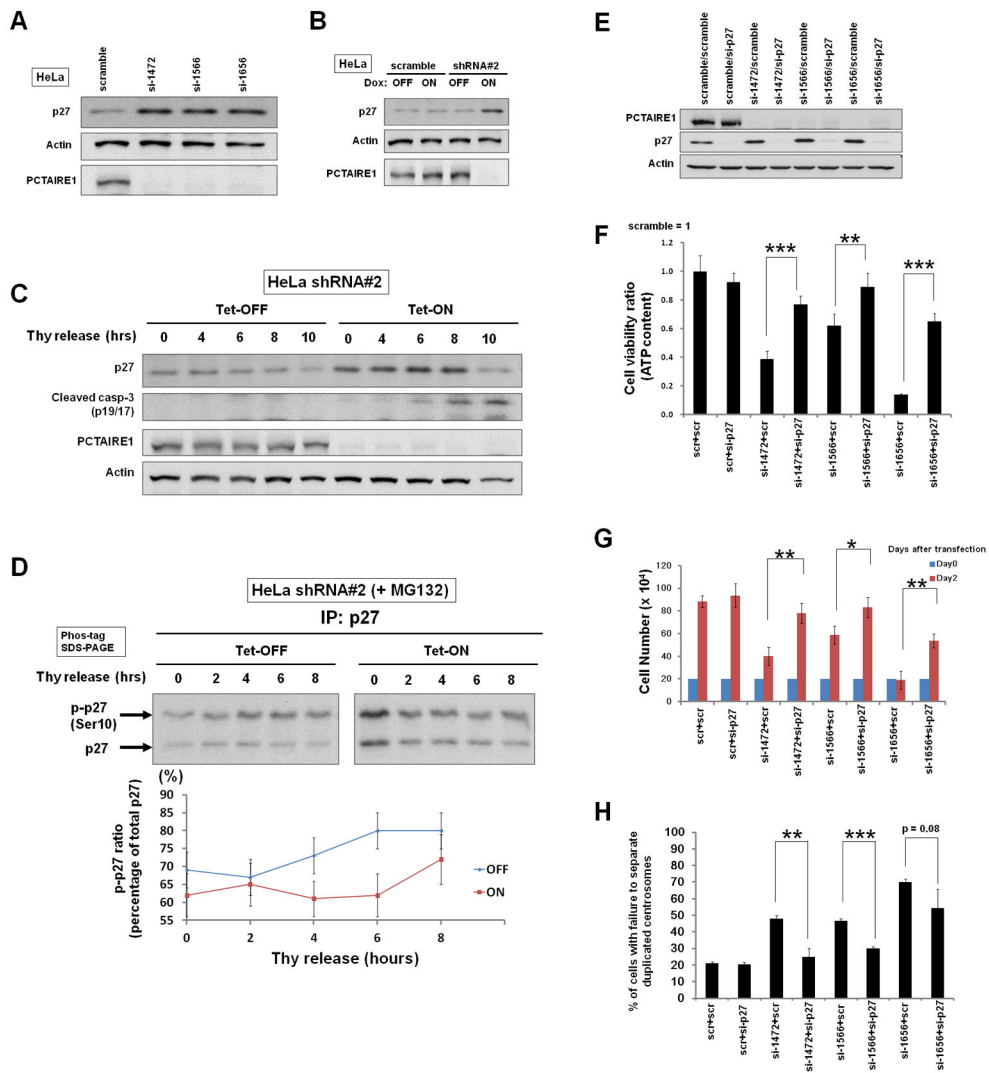(A) 2 days after siRNA transfection, cell lysates were analyzed by immunoblotting.

(B) PPC1 cells stably containing inducible shRNAs (#1, #2) were cultured for 2 days with (ON) or without (OFF) doxycycline. Protein lysates were analyzed by SDS-PAGE/ immunoblotting.

(C) p27 expression levels in resected xenograft tumors. Tumor lysates were harvested after doxycycline treatment for 12 days. Relative p27 levels were quantified by densitometry analysis. ** p< 0.01

(D) PPC1 cells stably containing inducible shRNA (#2) were cultured with (Tet-ON) or without (Tet-OFF) doxycycline. After 48 hours, cells were treated with 25 μg/ml cyclohexamide (CHX), and cell lysates were harvested at the indicated times. Relative p27

expression was quantified by densitometry analysis, and the results expressed as the percentage of p27 expression at 0 hour. *** $p < 0.001$

(E) 48 hours after siRNA transfection, cells were fractionated to yield cytosolic and nuclear compartments, which were analyzed by SDS-PAGE/immunoblotting.

Fig. 6. PCTAIRE1 regulates phosphorylation/degradation of p27 during S-M phases and p27 knockdown rescues PCTAIRE1 knockdown-mediated proliferation arrest

(A) 48 hours after siRNA transfection, cell lysates were analyzed by immunoblotting.

(B) HeLa cells with inducible shRNAs were cultured for 48 hours with (ON) or without (OFF) doxycycline. Protein lysates were analyzed by immunoblotting.

(C) HeLa cells with shRNAs (#2) were cultured for 48 hours with (ON) or without (OFF) doxycycline. Cells were synchronized by a double thymidine block. Cell lysates were subjected to immunoblot analysis.

(D) HeLa cells with shRNA (#2) were cultured for 2 days with (ON) or without (OFF) doxycycline, and synchronized by a double thymidine block. At 4 hours before cell lysate harvesting, MG132 (10 μM) was added to the media. Cell lysates were immunoprecipitated with rabbit anti-p27 antibody, and subjected to phos-tag SDS-PAGE, followed by immunoblotting with mouse anti-p27. Phosphorylated p27 (Ser10) was quantified by densitometry and normalized by total p27 expression (Mean ± SD; n = 3).

(E, F) PPC1 cells were transfected with scramble-control RNA, or siRNAs targeting PCTAIRE1 and p27 in various combinations as indicated (5 nM each, total siRNA

concentration was 10 nM). After 48 hours, cell lysates were analyzed by immunoblotting
(E). Cellular ATP levels were measured, with the data expressed as a ratio relative to cells
transfected with scramble-control RNA (mean ± SD; n = 3) (F). ** $p < 0.01$, *** $p < 0.001$
(G) 48 hours after siRNA transfection, the number of cells was counted (mean ± SD; n = 3).
* $p < 0.05$, ** $p < 0.01$

(H) The percentage of cells with unseparated duplicated centrosomes among prometaphase
cells was enumerated. *Columns*, mean (n = 3, determinations based on examination of 100
prometaphase cells); *bar*, SD. ** $p < 0.01$, *** $p < 0.001$
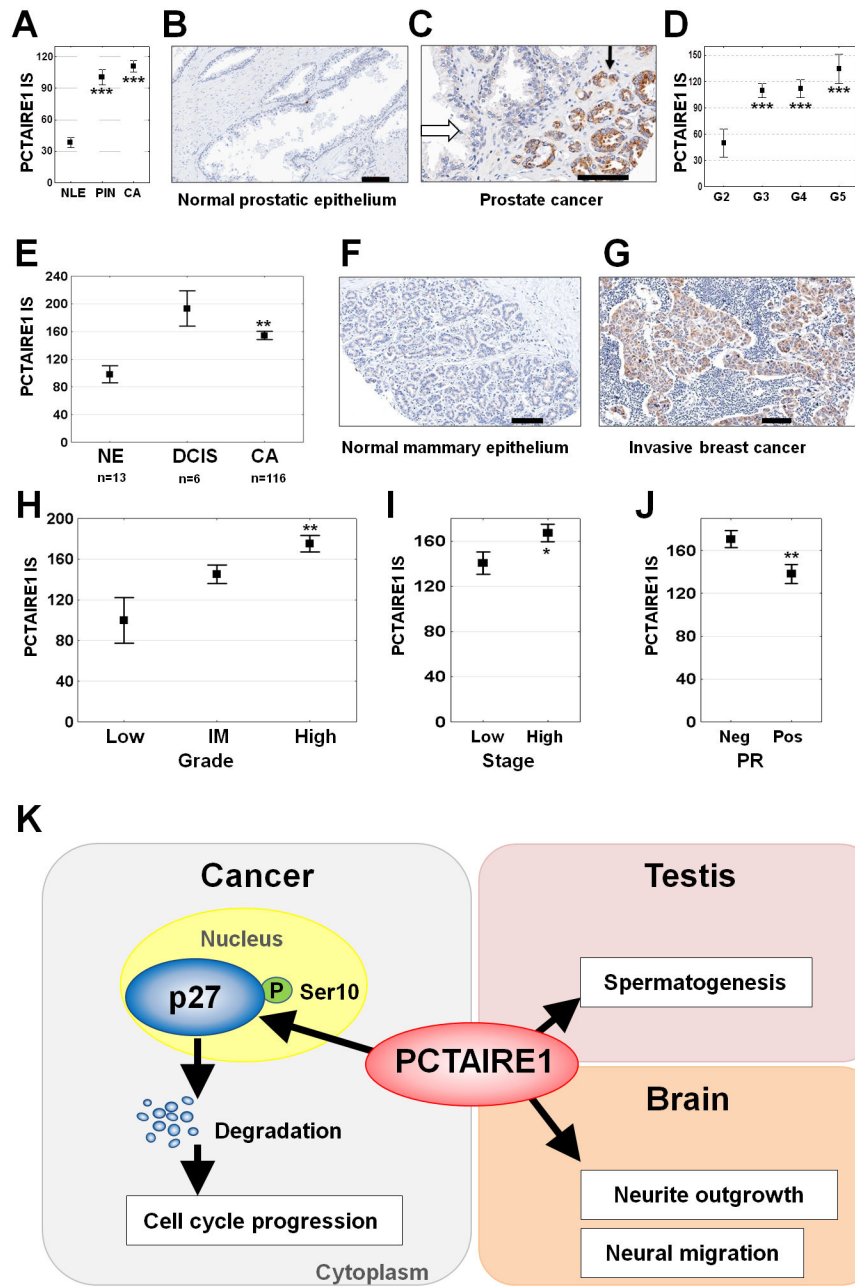
Fig. 7. Elevated levels of PCTAIRE1 in prostate and breast cancers

(A–D) PCTAIRE1 immunoscore (IS) data were generated from Tissue Microarrays. (A) Data (mean ± SEM) comparing normal luminal prostatic epithelium (NLE, n = 66 cores from 41 patients), prostatic intraepithelial neoplasia (PIN, n = 72 cores from 58 patients), and invasive prostate cancer (CA, n = 208 cores from 115 patients). *** p < 0.001 (B, C) Representative examples of PCTAIRE1 immunostaining results are provided for (B) normal prostatic epithelium and (C) prostate cancer (black and open arrows indicate tumor and adjacent nonmalignant tissue, respectively). Scale Bar = 100 μm. (D) Data (mean ± SEM) comparing Gleason grade 2–5 (G2–G5) among prostate cancer tumor specimens. *** p < 0.001, p values were determined using the ANOVA test.

(E–J) PCTAIRE1 immunohistochemistry results for breast cancer. PCTAIRE1 distribution was analyzed in normal mammary epithelium (NE, n = 13) (E, F), ductal carcinoma in situ (DCIS, n = 6) (E), and invasive cancer (CA, n = 116) (E, G–J). Associations between PCTAIRE1 immunoscore (IS) and tumor histologic grade (Low, intermediate (IM), High) (H), stage of disease (I & IIA = Low; IIB & IIIA = High) (I), and progesterone receptor (PR) (J) status were assessed using the ANOVA test. $* p < 0.05$, $** p < 0.01$, $*** p < 0.001$

(K) Model of PCTAIRE1 function. In normal tissues (right), PCTAIRE1 is required for spermatogenesis and neuron differentiation. In cancer cells (left), PCTAIRE1 phosphorylates p27, thereby promoting p27 degradation.